Electronic Supplementary Material (ESI) for Nanoscale.

Supplementary Information

Hierarchically porous activated carbons prepared via a dissipative process: high-capacity cathode for Li ion capacitors

Qi Cao, Guoqing Ning, Fan Yang, Ye Wang, Bofeng Li, Xinlong Ma*

State Key Laboratory of Heavy Oil Processing, China University of Petroleum, Beijing, 102249, China.

*Corresponding author E-mail: ninggq@qq.com

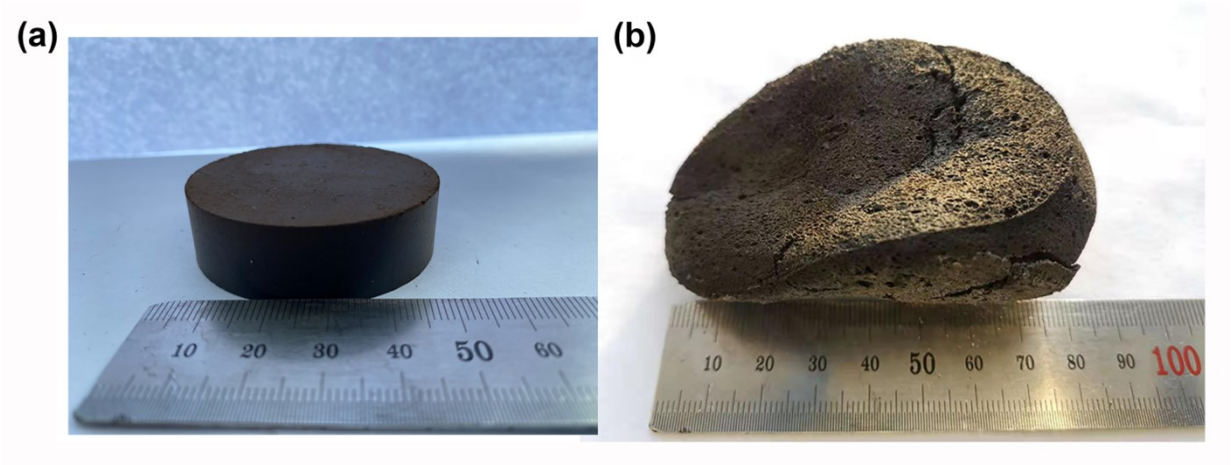

Fig. S1 The digital images of the asphalt-KOH tablet (a) before and (b) after the 800 ˚C calcination.

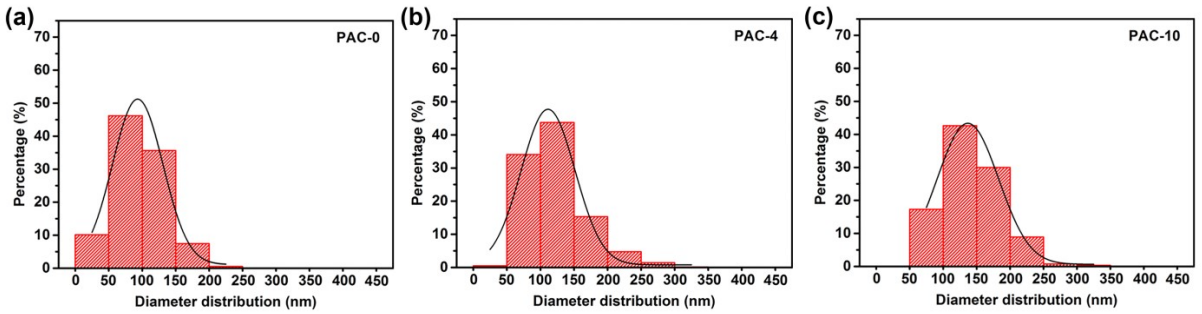

Fig. S2 Pore diameter distribution statistics (based on SEM images) of PACs prepared at the tableting pressure of 0 (a), 4 (b) and 10 MPa (c).

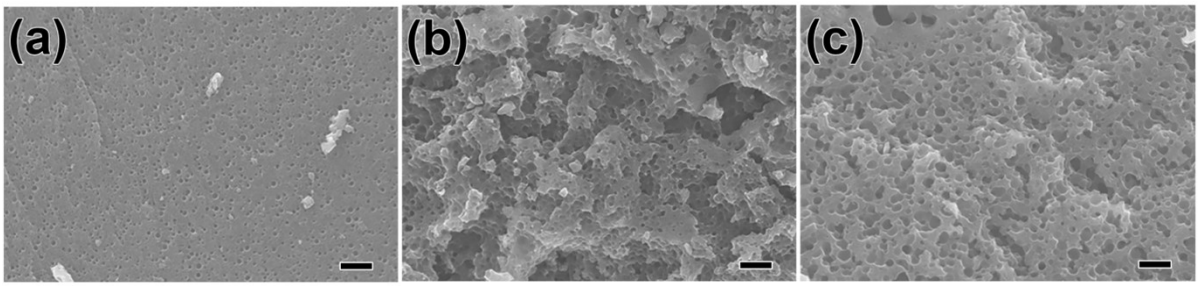

Fig. S3 SEM images of PACs prepared at the tableting pressure of 0 (a), 4 (b) and 10 MPa (c) with a KOH to asphalt ratio of 1. Scale bars, 500 nm.

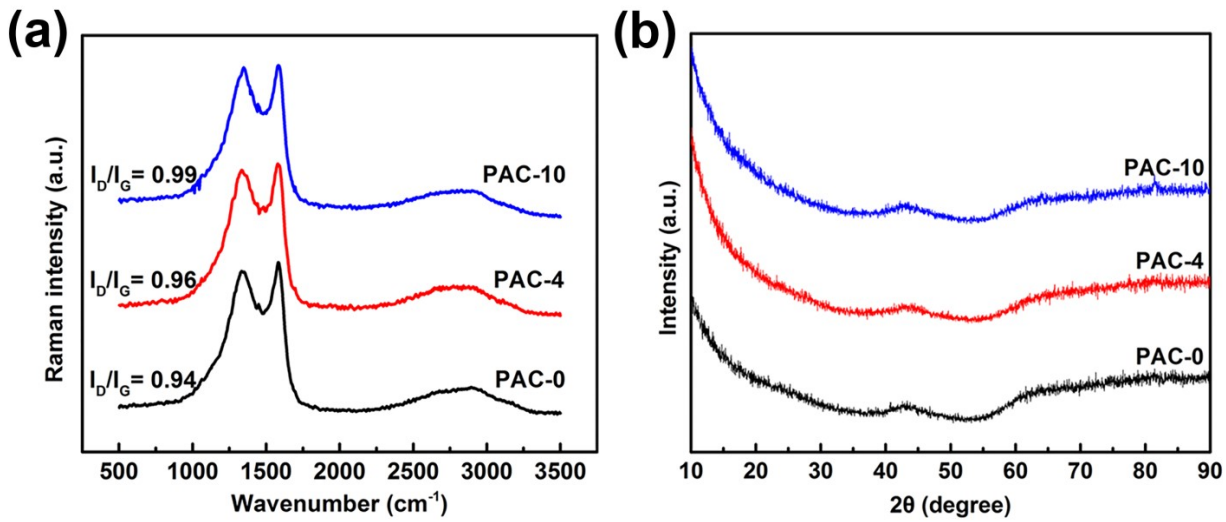

Fig. S4 (a) Raman spectra and (b) XRD patterns of PAC-0, PAC-4 and PAC-10.

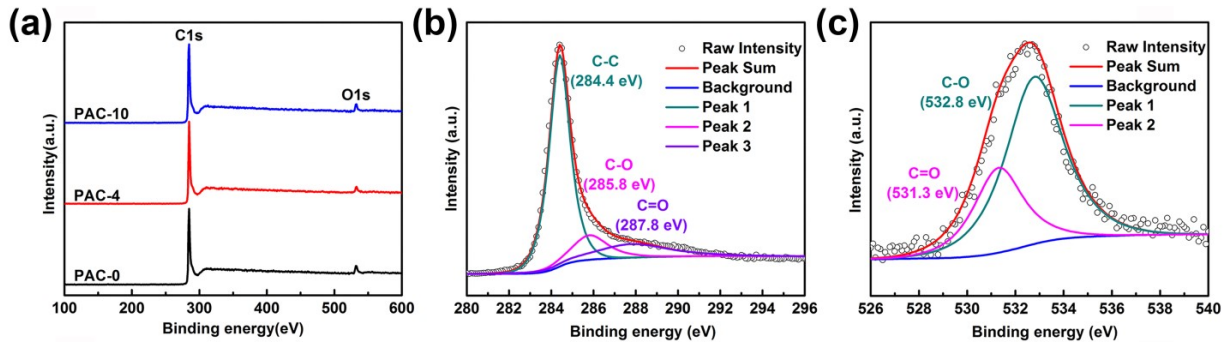

Fig. S5 (a) XPS survey spectra of PAC-0, PAC-4 and PAC-10. High resolution (b) C1s and (c) O1s spectra of PAC-10.

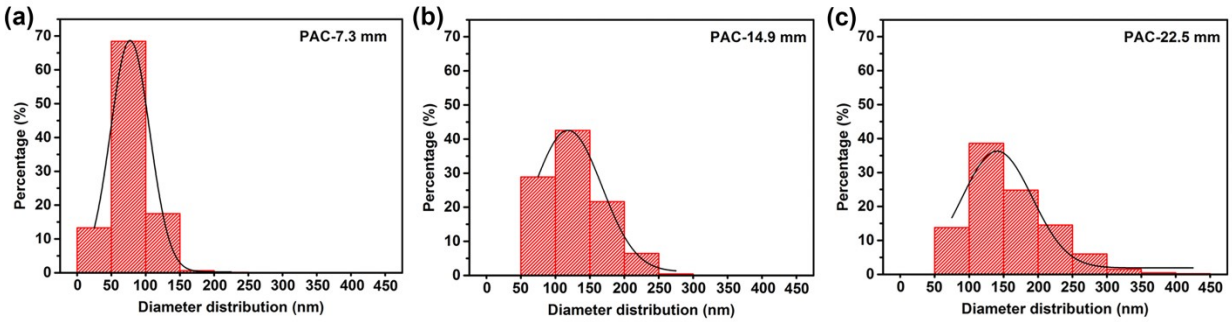

Fig. S6 Pore diameter distribution statistics (based on SEM images) of PACs prepared at the tablet thickness of 7.3 (a), 14.9 (b) and 22.5 mm (c).

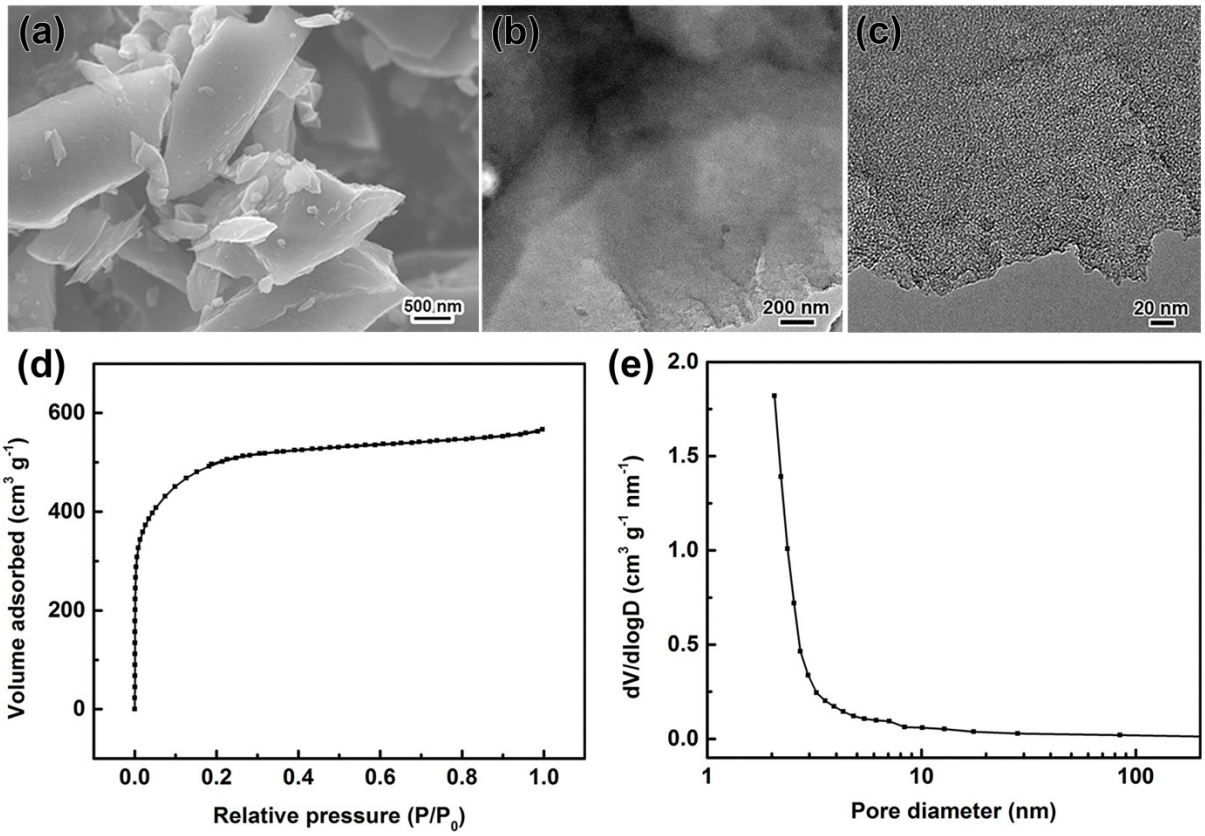

Fig. S7 (a) SEM, (b) TEM and (c) HR-TEM images of CAC. (d) N_2 adsorption/desorption isotherm and (e) BJH pore size distribution of CAC.

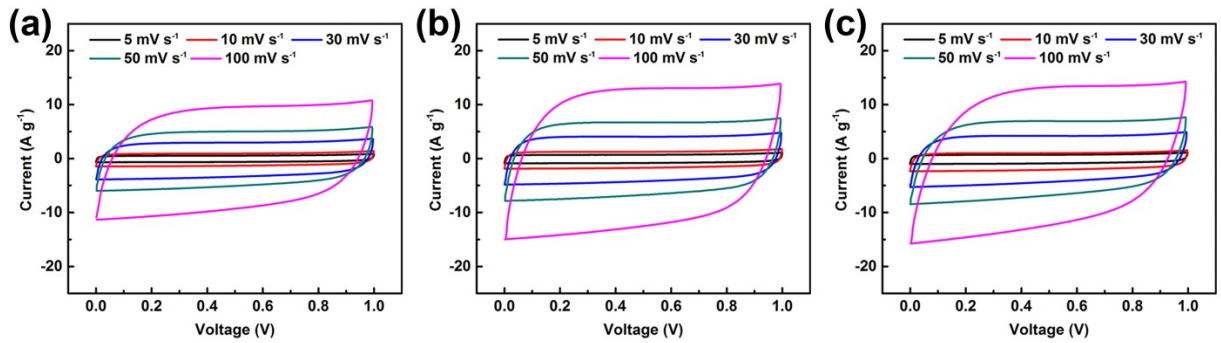

Fig. S8 CV curves of (a) CAC, (b) PAC-0 and (c) PAC-4 at different scan rates as electrodes for SSCs.

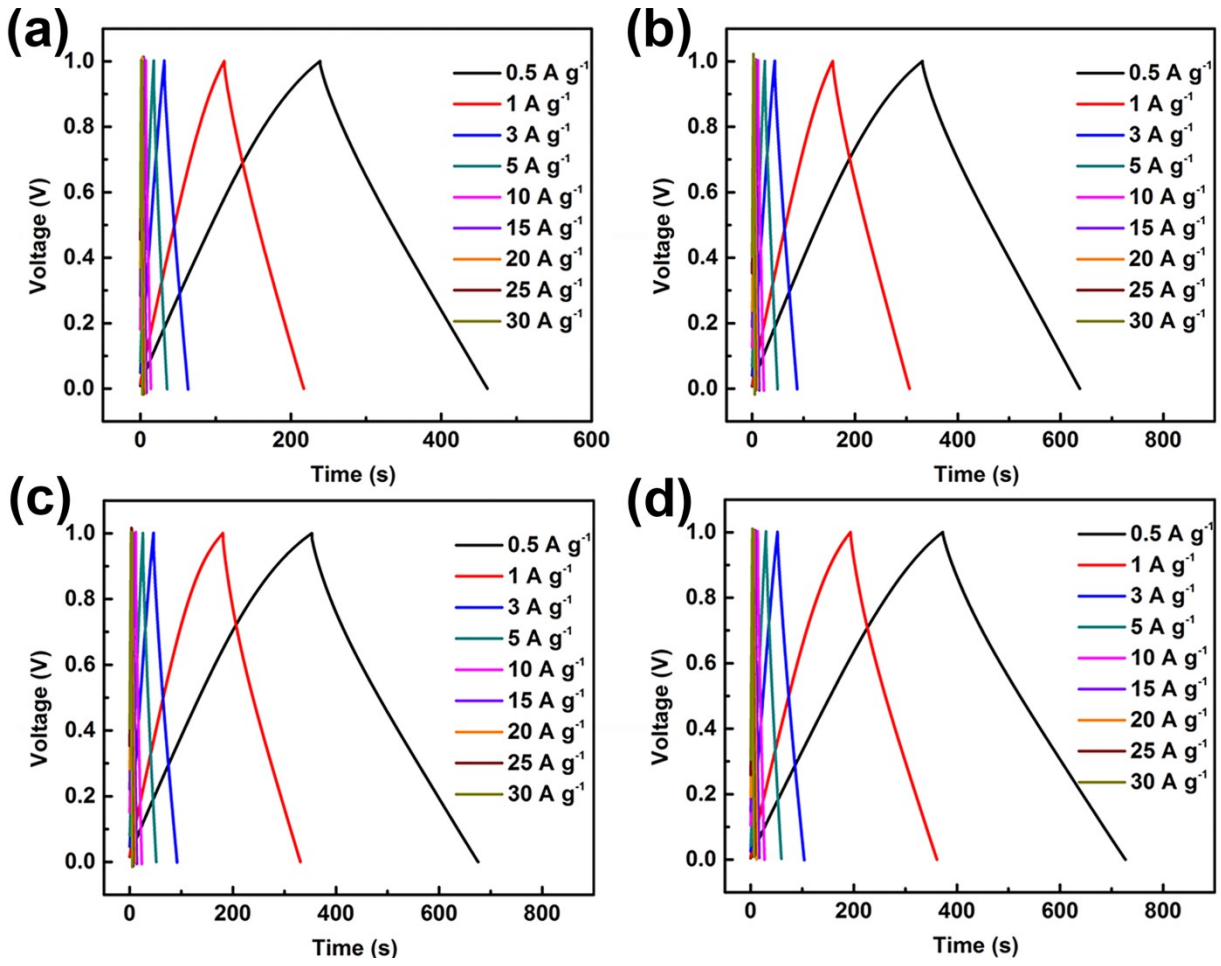

Fig. S9 Galvanostatic charge/discharge curves of (a) CAC, (b) PAC-0, (c) PAC-4 and (d) PAC-10 at different current densities as electrodes for SSCs.

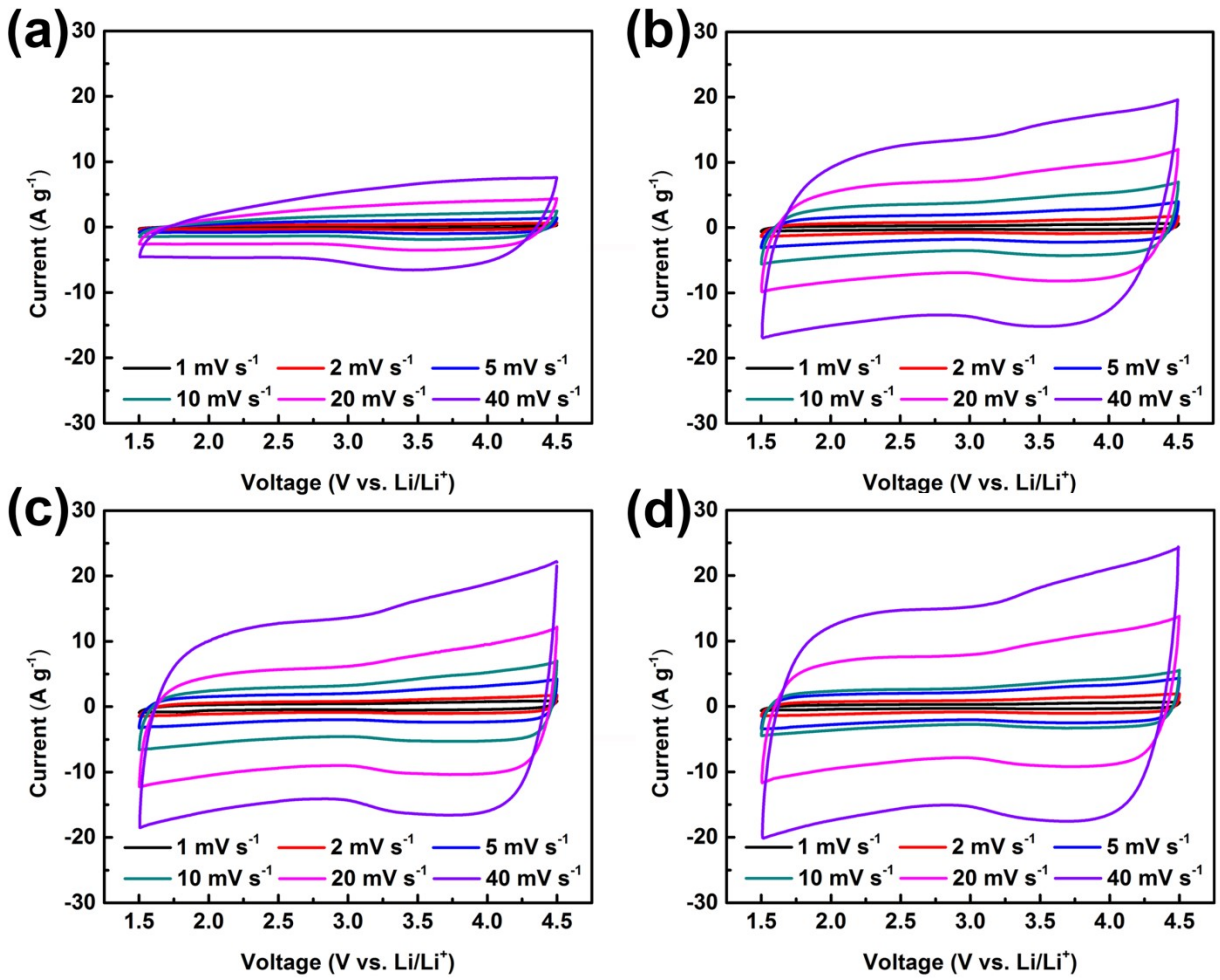

Fig. S10 CV curves of (a) CAC, (b) PAC-0, (c) PAC-4 and (d) PAC-10 at different scan rates as cathodes for LICs.

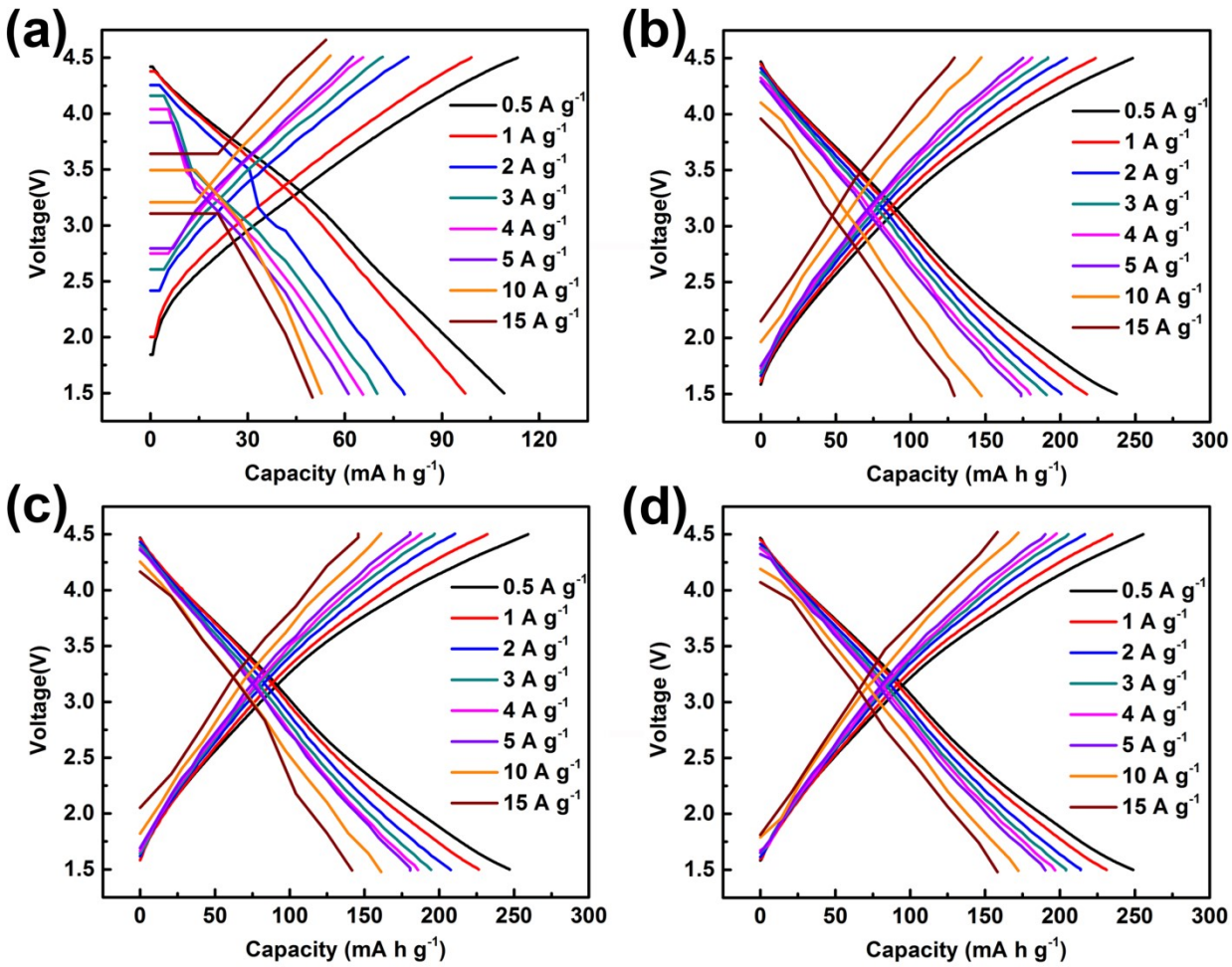

Fig. S11 Charge/discharge curves of (a) CAC, (b) PAC-0, (c) PAC-4 and (d) PAC-10 at different current densities as cathodes for LICs.

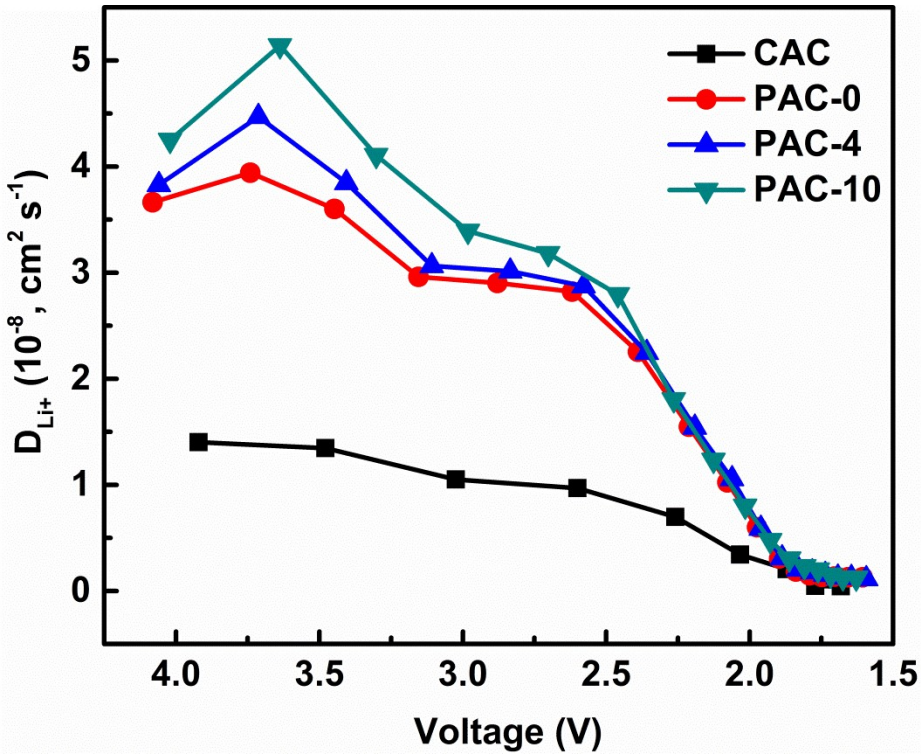

Fig. S12 Li^+ diffusion coefficients in the CAC, PAC-0, PAC-4 and PAC-10 cathodes.

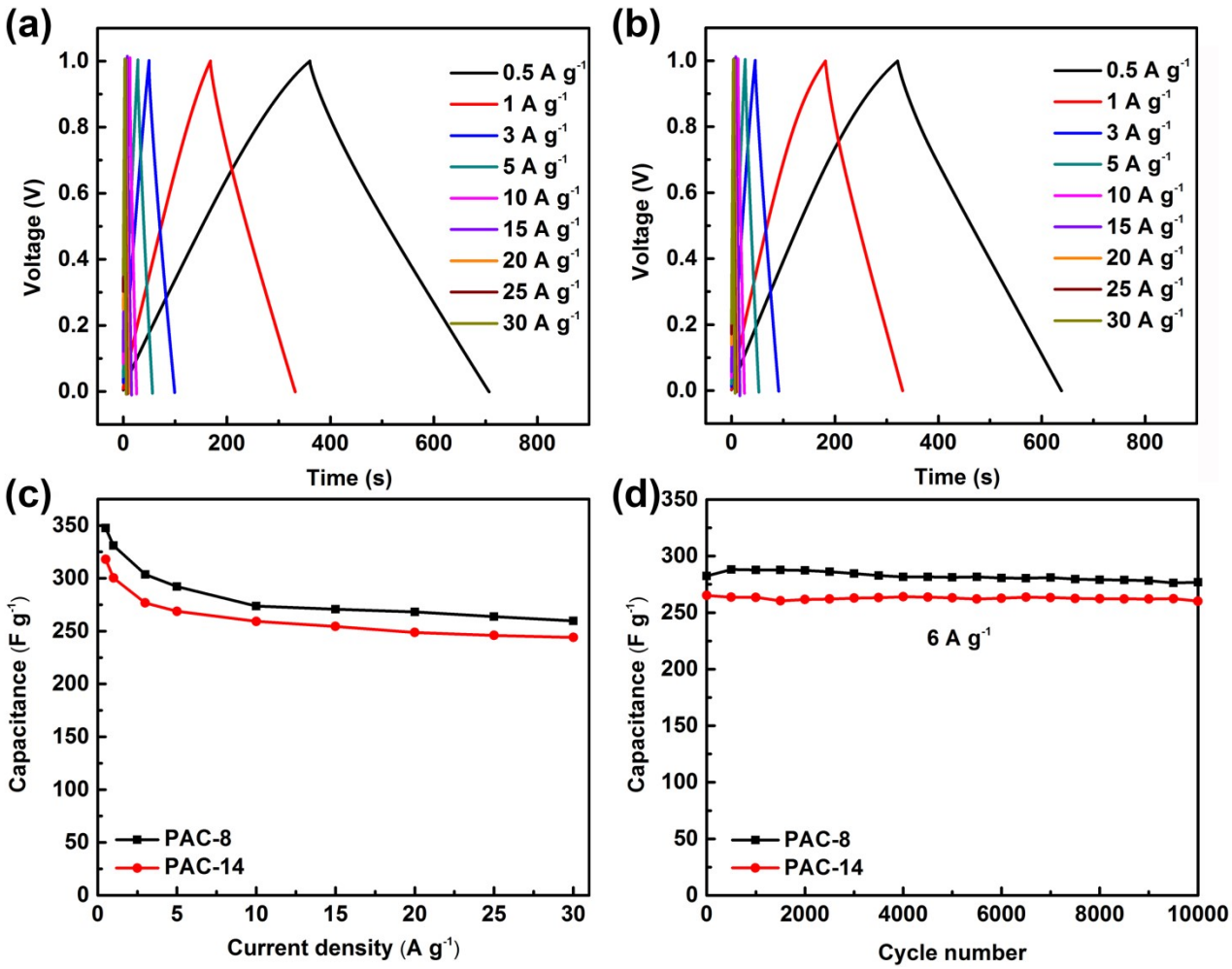

Fig. S13 Galvanostatic charge/discharge curves of (a) PAC-8 and (b) PAC-14 electrodes at different current densities. (c) Rate capabilities and (d) cycling performances at 6 A g^{-1} of PAC-8 and PAC-14 electrodes for SSCs in 6M KOH electrolyte.

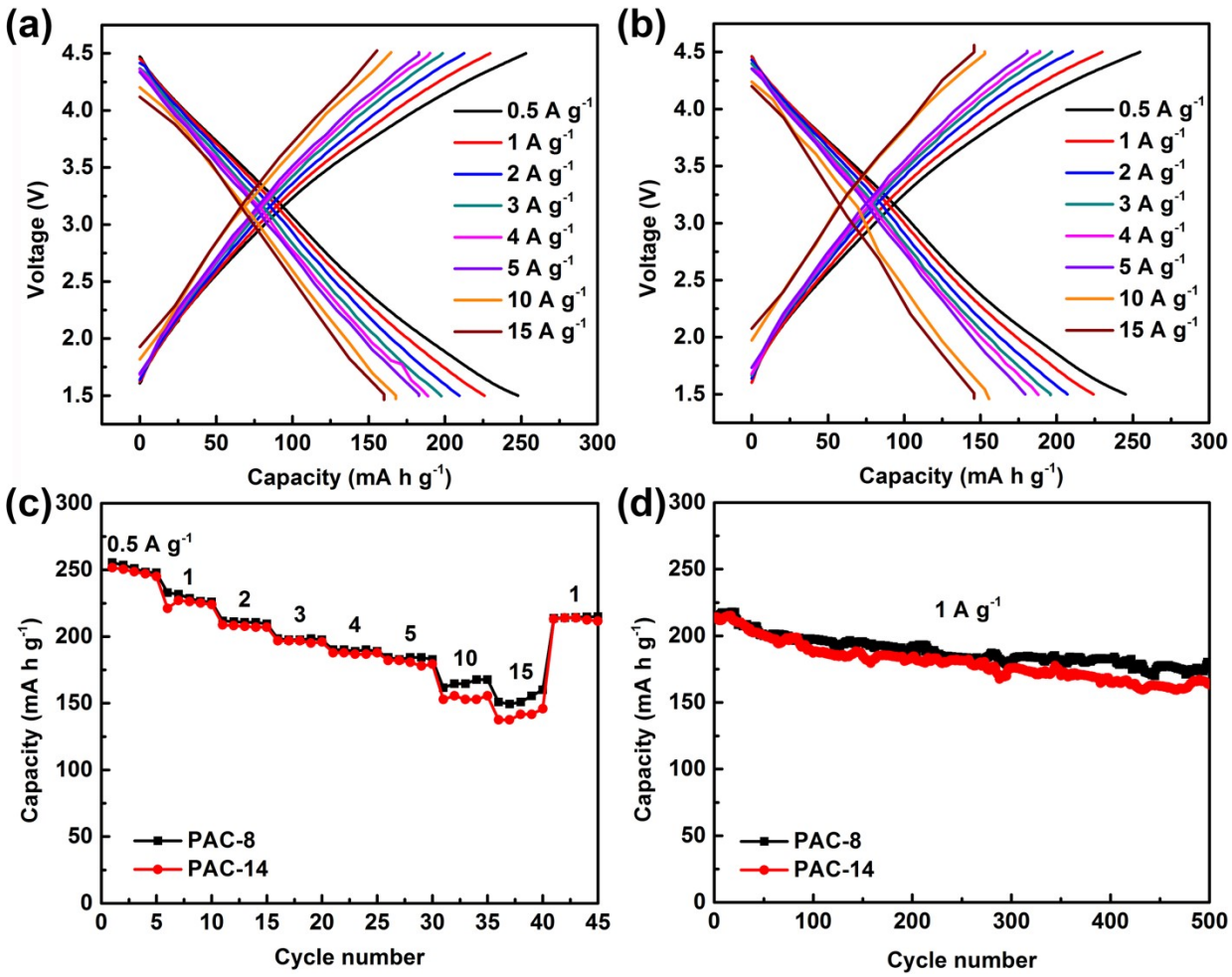

Fig. S14 Charge/discharge curves of (a) PAC-8 and (b) PAC-14 cathodes at different current densities. (c) Rate capabilities and (c) cycling performances at 1 A g^{-1} of PAC-8 and PAC-14 cathodes for LICs.

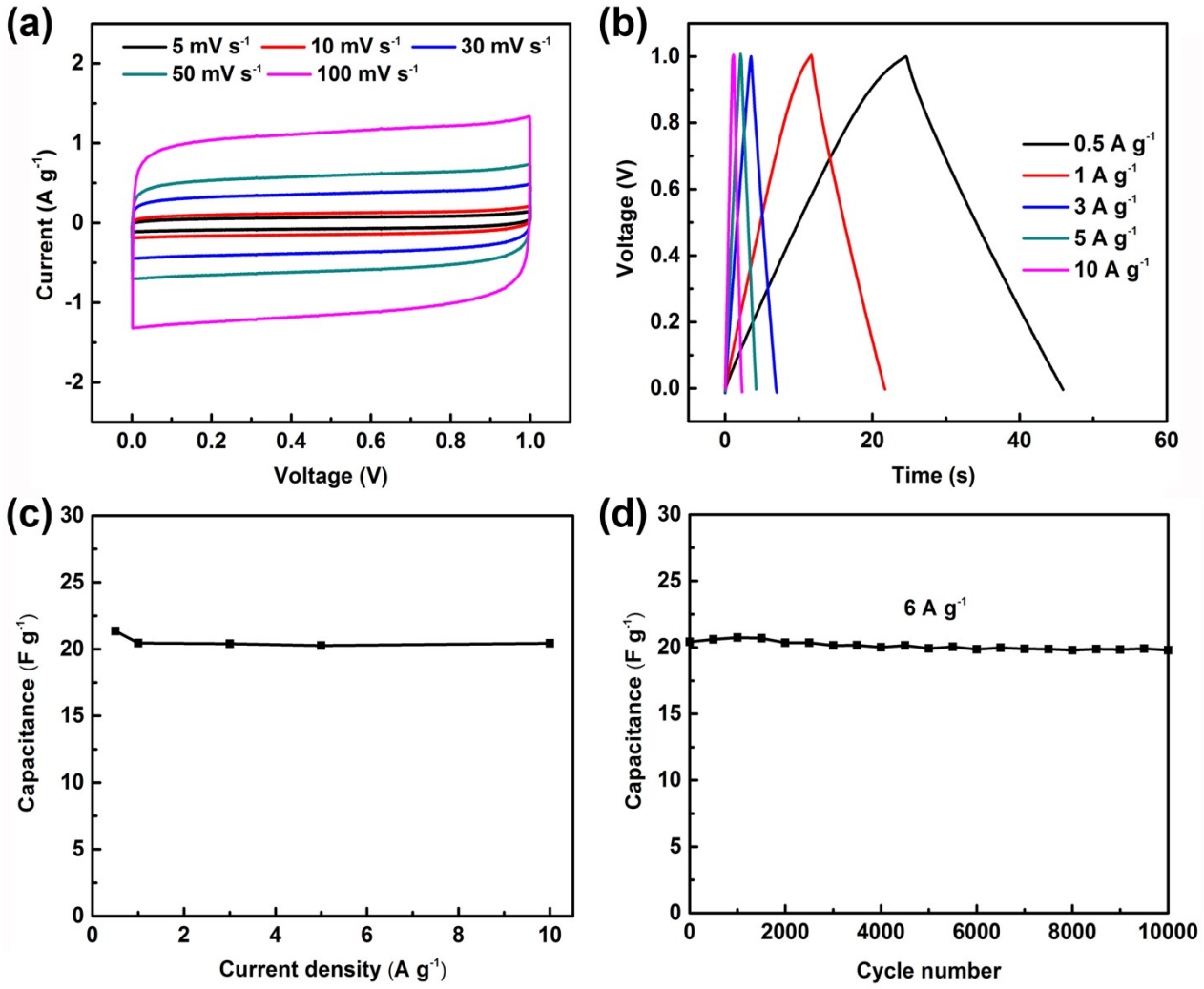

Fig. S15 (a) CV profiles at diffetent scan rates, (b) galvanostatic charge/discharge curves at different current densities, (c) rate capability and (d) cycling performance at 6 A g^{-1} of PAC-10-0KOH electrode for SSCs in 6M KOH electrolyte.

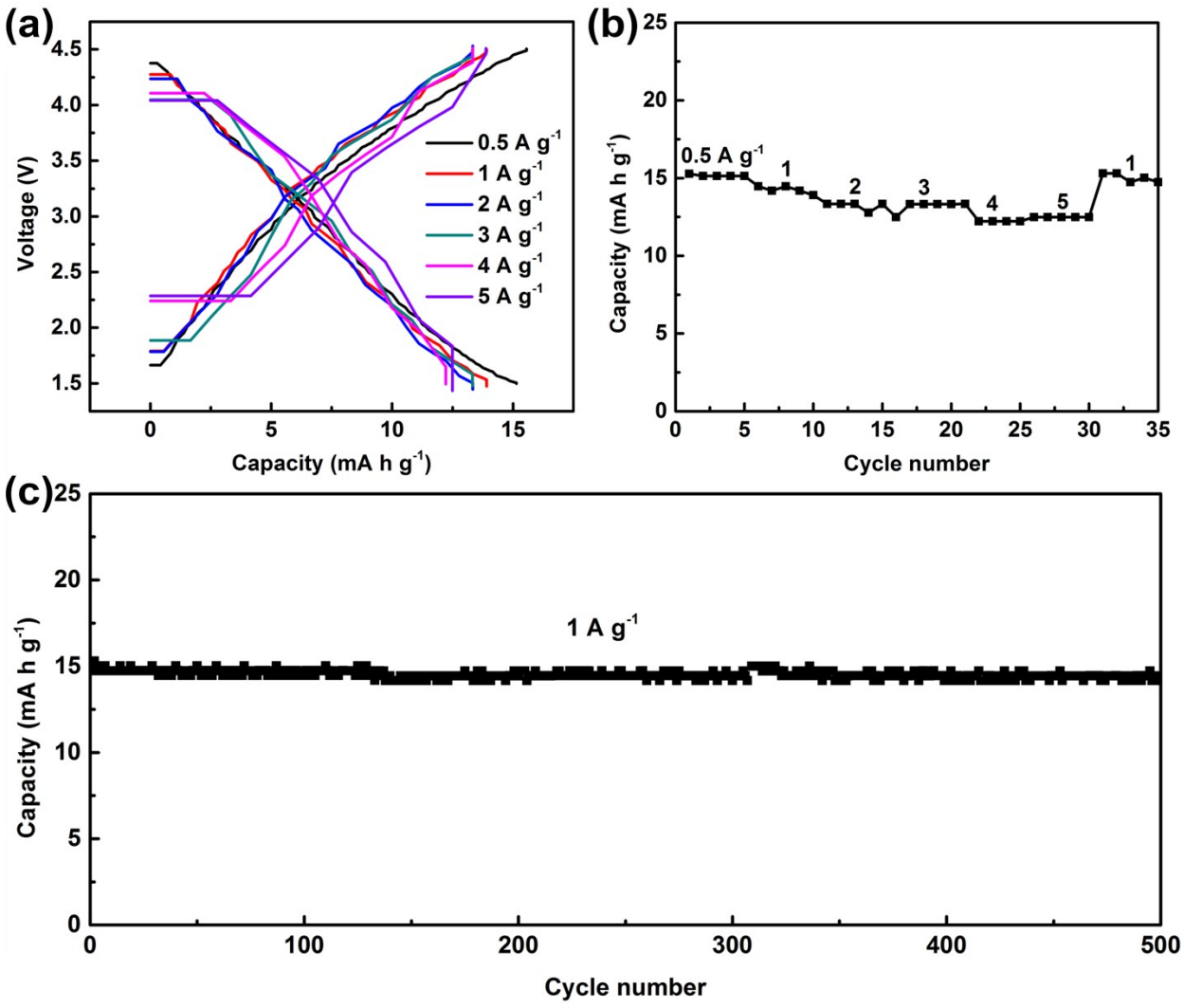

Fig. S16 (a) Charge/discharge curves at different current densities, (b) rate capability and (c) cycling performance at 1 A g^{-1} of PAC-10-0KOH cathode for LICs.

Table S1 Pore structure parameters of CAC and PACs prepared at different tabletting pressures, different tablet thicknesses and without adding KOH.

Sample	S_{BET} (m^2 g^{-1})	V_t (cm^3 g^{-1})	V_{micro} (cm^3 g^{-1})	V_{meso} (cm^3 g^{-1})	V_{meso}/V_t %	D_a (nm)
CAC	1627	0.88	0.72	0.16	18.2	2.15
PAC-0	3015	1.63	1.23	0.40	24.5	2.17
PAC-4	3099	1.79	1.25	0.54	30.2	2.31
PAC-8	3174	1.84	1.28	0.56	30.4	2.32
PAC-10	3211	2.02	1.25	0.77	38.1	2.52
PAC-14	3074	1.82	1.24	0.58	31.9	2.36
PAC-7.3 mm	3015	1.67	1.23	0.44	26.3	2.21
PAC-14.9 mm	3174	1.84	1.28	0.56	30.4	2.32
PAC-22.5 mm	2931	1.90	1.15	0.75	39.5	2.60
PAC-10-0KOH	37	0.03	-	-	-	2.70

Note: The sample PAC-8 and PAC-14.9 mm represent the same PAC.

Table S2 Pore structure parameters of PAC-10 samples prepared at different heating rates of 5, 10 and 20 ˚C min^{-1}.

Sample	S_{BET} (m^2 g^{-1})	V_t (cm^3 g^{-1})	V_{micro} (cm^3 g^{-1})	V_{meso} (cm^3 g^{-1})	V_{meso}/V_t %	D_a (nm)
PAC-10-5 ˚C min^{-1}	3075	1.77	1.24	0.53	29.9	2.31
PAC-10-10 ˚C min^{-1}	3211	2.02	1.25	0.77	38.1	2.52
PAC-10-20 ˚C min^{-1}	3182	1.85	1.21	0.64	34.6	2.33

Table S3 Surface compositions of PAC-0, PAC-4 and PAC-10 samples (XPS spectra).

Sample	C (at%)	O (at%)
PAC-0	94.98	5.02
PAC-4	95.83	4.17
PAC-10	95.96	4.04

Table S4 Comparison of the electrochemical performances of some previously reported AC materials when measured in a two-electrode system using 6M KOH aqueous electrolyte.

Sanples	SSA (m^2 g^{-1})	Voltage window (V)	Specific capacitance		Cycling stability			Ref.
			Current density (A g^{-1})	Capacitance (F g^{-1})	Current density (A g^{-1})	Cycle number	Capacitance retention (%)	
$HPC_{20\text{-}800}$	2102	0-1.0	0.4	244	5	10000	91.1	[44]
SRPC-4K	2143	0-1.0	0.5	276	5	10000	98	[45]
AHPC	2650	0-1.0	0.5	310	10	10000	95	[46]
GHC-17	2818	0-1.0	0.5	427	4.5	5000	94	[47]
HGPC-A	1009	0-1.0	0.5	203	10	10000	88.5	[48]
WSPC	2465	0-1.4	0.5	207	5	8000	90.2	[49]
CS3-T800	2812	0-1.0	1	302	20	5000	95.0	[50]
$HPC_{2\text{-}700}$	1214	0-1.0	1	260	5	5000	85.6	[51]
HPCNs-g	1213	0-1.0	1	221	4	10000	100.4	[52]
HPC	1356	0-1.0	1	205	10	30000	99.55	[53]
PAC-10	3211	0-1.0	0.5	356	6	10000	100	This work
			1	338				

Table S5 Typical half-cell capacity of AC materials as a positive electrode for LICs based on a non-aqueous $LiPF_6$ electrolyte.

Samples	SSA (m^2 g^{-1})	Voltage window (V)	Current density (A g^{-1})	Specific capacity (mA h g^{-1})	Ref.
SFAC-3	3104	2.0-4.0	0.5	78	[59]
eAC-900	3250	2.0-4.5	0.4	127	[60]
CPAC-5	3011	2.0-4.5	0.5	107	[61]
LDAC	2808	2.0-4.5	0.5	130	[62]
AC	1600	2.0-4.5	0.5	97	[63]
HPC-800	3285	2.0-4.2	0.5	104	[64]
NDPC-0.5	1506	2.0-4.5	0.5	78	[65]
APDC-700	2449	2.0-4.5	0.5	147	[66]
PCNs-800	1317	2.0-4.5	0.5	78	[67]
KAC-6	2719	1.5-4.5	0.5	167	[68]
PAC-10	3211	1.5-4.5	0.5	251	This work
			15	158	